J|A|C|S
ARTICLES
Published on Web 10/09/2002

Structure and Stereochemistry of a New Cytotoxic Polychlorinated Sulfolipid from Adriatic Shellfish

Patrizia Ciminiello,*,† Carmela Dell'Aversano,† Ernesto Fattorusso,*,† Martino Forino,† Silvana Magno,† Massimo Di Rosa,‡ Angela Ianaro,‡ and Roberto Poletti§

Contribution from Dipartimento di Chimica delle Sostanze Naturali, Università degli studi di Napoli "Federico II", via D. Montesano 49, 80131, Napoli, Italy, Dipartimento di Farmacologia Sperimentale, Università degli studi di Napoli "Federico II", via D. Montesano 49, 80131, Napoli, Italy, and Centro di Ricerche Marine, via A. Vespucci 2, 47042 Cesenatico (FC), Italy

Received May 24, 2002

Abstract: A detailed analysis of the causative toxins contained in the hepatopancreas of toxic mussels from the northern Adriatic sea has been carried out. Along with some DSP (diarrhetic shellfish poisoning) type toxins, such as okadaic acid, yessotoxin, and their derivatives, which are involved in a number of human intoxications throughout the world, we have now isolated a new cytotoxin, a polychlorinated sulfolipid **1**, whose gross structure has been elucidated by spectral analysis, including various 2D NMR techniques. The relative stereochemistry of **1** was elucidated by successful application of the *J*-based configuration analysis developed for acyclic compounds using carbon−proton spin-coupling constants ($^{2,3}J_{C,H}$) and proton−proton spin-coupling constants ($^{3}J_{H,H}$); its absolute stereochemistry was established by the Mosher method. Compound **1** possesses in vitro cytotoxicity against WEHI 164 and RAW 264.7 cells.

Introduction

In the past decades, marine toxins have aroused scientists' growing interest due to their involvement in human poisonings, occurring with alarming frequency throughout the world, and to socioeconomic impacts of these incidents. As biotoxins move up through marine food webs, they can have a broad spectrum of effects on marine animals in inshore, offshore, pelagic, and benthic habitats.[1] A wide variety of animals can accumulate biotoxins and act as intermediate vectors to consumers at higher trophic levels. Certain groups of animals, as direct consumers of microalgae, have received primary attention with regard to specific biotoxins. The best-known examples are filter-feeding bivalve mollusks as vectors for paralytic shellfish poisoning (PSP), neurotoxic shellfish poisoning (NSP), diarrhetic shellfish poisoning (DSP), and amnesic shellfish poisoning (ASP).[2]

In our ongoing efforts toward finding novel marine toxins we have been investigating toxic shellfish of the Northwestern Adriatic sea. In this area, DSP outbreaks associated with harmful algae blooms have been recognized as a problem since 1989, when the first case of human gastroenteritis was related to the simultaneous presence of known producers of DSP toxins both in seawater and hepatopancreas of mussels.[3] Initially okadaic acid (OA)[4] and dinophysistoxin-1 (DTX-1)[5] were pointed out as the causative agents. Successively, human intoxication was related to the presence of yessotoxin (YTX) and its analogues,[6−10] while OA and DTX-1 were no longer detected.

Very recently we have reported isolation and stereostructure elucidation of a cytotoxic polychlorinated sulfolipid, which was shown to be contained in toxic shellfish together with YTXs.[11] Chlorine-substituted docosane and tetracosane disulfates, whose structures were assigned devoid of stereochemical details, have

* To whom correspondence should be addressed. Phone: 0039-081-678 507. Fax: 0039-081-678 552. E-mail for E.F.: fattoru@unina.it. E-mail for P.C.: ciminiel@unina.it.

† Dipartimento di Chimica delle Sostanze Naturali, Università degli studi di Napoli "Federico II".

‡ Dipartimento di Farmacologia Sperimentale, Università degli studi di Napoli "Federico II".

§ Centro di Ricerche Marine.

(1) Hashimoto, Y. *Marine Toxins and Other Bioactive Marine Metabolites*; Japan Scientific Societies Press: Tokyo, 1979.

(2) (a) Shumway, S. E. *J. World Aquacult. Soc.* **1990**, *21*, 65. (b) Hallegraff, G. M. *Phycologia* **1993**, *32*, 79. (c) Yasumoto, T. In *Toxic Marine Phytoplankton*; Graneli, E., Sundstron, B., Edler, L., Anderson, D. M., Eds.; Elsevier: Amsterdam, 1990; pp 3−8. (d) Yasumoto, T.; Murata, M. *Chem. Rev.* **1993**, *93*, 1897.

(3) (a) Boni, L.; Mancini, L.; Milandri, A.; Poletti, R.; Pompei, M.; Viviani R. In *Marine Coastal Eutrophication*; Vollenweider, R. A., Marchetti, R., Viviani, R., Eds.; Elsevier: Amsterdam, 1992; pp 419−426. (b) Boni, L.; Milandri, A.; Poletti, R.; Pompei M. In *Toxic Phytoplankton Blooms in the Sea*; Smayda, T. J.; Shimizu Y., Eds.; Elsevier: Amsterdam, 1993; pp 475−481.

(4) Fattorusso, E.; Ciminiello, P.; Costantino, V.; Magno, S.; Mangoni, A.; Milandri, A.; Poletti, R.; Pompei, M.; Viviani, R. *Mar. Poll. Bull.* **1992**, *24*, 234.

(5) (a) Draisci, R.; Lucentini, L.; Giannetti, L.; Stacchini, A. *Riv. Sci. Aliment.* **1993**, *4*, 443. (b) Draisci, R.; Lucentini, L.; Giannetti, L.; Boria, P.; Stacchini, A.; Poletti, R. *Riv. Soc. Ital. Sci. Aliment.* **1996**, *25*, 7.

(6) Ciminiello, P.; Fattorusso, E.; Forino, M.; Magno, S.; Poletti, R.; Satake, M.; Viviani, R.; Yasumoto, T. *Toxicon* **1997**, *35*, 177.

(7) Ciminiello, P.; Fattorusso, E.; Forino, M.; Magno, S.; Poletti, R.; Viviani, R. *Toxicon* **1999**, *37*, 689.

(8) Ciminiello, P.; Fattorusso, E.; Forino, M.; Magno, S.; Poletti, R.; Viviani, R. *Tetrahedron Lett.* **1998**, *39*, 8897.

(9) Ciminiello, P.; Fattorusso, E.; Forino, M.; Poletti, R.; Viviani, R. *Eur. J. Org. Chem.* **2000**, *2*, 291.

(10) Ciminiello, P.; Fattorusso, E.; Forino, M.; Poletti, R.; Viviani, R. *Chem. Res. Toxicol.* **2000**, *13*, 770.

(11) Ciminiello, P.; Fattorusso, E.; Forino, M.; Di Rosa, M.; Ianaro A.; Poletti, R.; . *J. Org. Chem.* **2001**, *66*, 578.

10.1021/ja0207347 CCC: $22.00

Chart 1

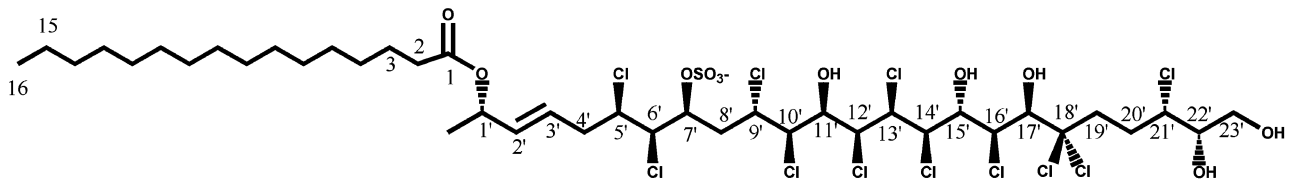

1

been previously reported in the microalgae *Ochromonas danica* and *Poterioochromonas mahlamensis* (*P. mahlamensis*; Chrysophyta, Chrysophyceae),[12] where they represent almost half of the total membrane lipids. The chlorosulfolipids of *P. malhamensis* were found to be predominantly of the tetracosane-1, 14-diol disulfate variety[13] and displayed broad-spectrum antimicrobial activity.[14]

To date, the presence of this type of compound appears to be not incidental in Adriatic shellfish, as we have now isolated a new cytotoxic polychlorinated sulfolipid from toxic mussels (hexadecanoic acid 5′,6′,9′,10′,12′,13′,14′,16′,18′,18′,21′-undecachloro-11′,15′,17′,22′,23′-pentahydroxy-1′-methyl-7′-sulfooxytricos-2′-enyl ester, **1**, Chart 1); herein we report its isolation, total stereostructure determination, and cytotoxic activity evaluation.

Results and Discussion

Toxic mussels *Mytilus galloprovincialis* were collected in October 1999 from one shellfish cultivation site located along the Emilia Romagna coasts of Italy, when routine control testing had shown mussels to be positive for DSP toxins by the official mouse bioassay.[15] Only the digestive glands of the animals were used for the bioassay-guided isolation of **1**, as reported in the Experimental Section.

The negative ion ESIMS spectrum of **1** contained a very intense pseudomolecular ion cluster at *m*/*z* 1139, 1141, 1143, 1145, 1147, 1149, 1151. The complete molecular formula $C_{40}H_{66}O_{11}SCl_{11}$, implying 2° of unsaturation, was established from the negative ion HRESIMS spectrum (measured mass *m*/*z* 1141.0936; calculated 1141.0870 for $C_{40}H_{66}O_{11}S^{35}Cl_{10}{}^{37}Cl$, error max 10 ppm). The molecular formula was corroborated by NMR spectroscopy (Table 1) and by comparison of the above cluster of peaks with a simulated molecular ion pattern of $C_{40}H_{66}O_{11}SCl_{11}$, which resulted in being fully superimposable.

The combined analysis of ^{1}H,^{13}C NMR, DEPT, and HMQC spectra of **1** showed that 38 carbon atoms were protonated, 36 being of sp^3 type (2 methyls, 19 methylenes, and 15 methines) and the remaining two sp^2 methine carbons; these latter signals evidenced the presence in **1** of a 1,2-disubstituted carbon−carbon double bond (see Table 1). The remaining two carbons were unprotonated and resonated in the ^{13}C NMR spectrum at δ 97.6 and δ 174.1, respectively. This latter signal pointed to the presence of an ester functionality in the molecule, thus accounting for two of the 11 oxygen atoms of the molecule. Another four oxygens were assumed to belong to a sulfate group, whose presence was evidenced by the absorptions at ν_{max} 1240, 1220, and 820 cm^{-1} in the IR spectrum, as well as by intense fragment ions at *m*/*z* 97 $[HSO_4]^-$ and 80 $[SO_3]^-$ in the MSMS spectrum (negative ion mode). The remaining five oxygens were part of five hydroxyl groups, as evidenced by the peracetylated derivative of **1**, whose mass and ^{1}H NMR spectra, as reported below, pointed to five acetyl groups being incorporated in the molecule.

The whole of the above data showed all the functionalities present in the molecule and, in addition, accounted for the two formal unsaturations implied by the molecular formula, thus pointing to the acyclic nature of **1**.

The ^{1}H NMR spectrum of **1** exhibited a number of overlapped signals in the mid-field region which prevented us from an easy determination of its planar structure through the connectivities present in the 2D ^{1}H−^{1}H NMR spectra. Consequently, the determination of the gross structure of the molecule was carried out on the peracetylated compound **2**, whose ^{1}H NMR spectrum showed a better dispersion of the signals, especially in the critical mid-field region. Each proton signal was associated with the corresponding carbon signal in the ^{13}C NMR spectrum through a HMQC experiment.

ESIMS spectrum of **2** (Chart 2) showed a pseudomolecular ion cluster of peaks at *m*/*z* 1349, 1351, 1353, 1355, 1357, 1359, 1361, which, together with ^{1}H and ^{13}C NMR data (Table 1), indicated a molecular formula $C_{50}H_{76}O_{16}SCl_{11}$, corresponding to a pentaacetyl derivative of **1**.

Analysis of ^{1}H−^{1}H COSY and HOHAHA spectra of **2** established two sequences of ^{1}H spin systems for the highly functionalized alcoholic portion of the molecule, the first of which spanned from Me−C1′ to C17′ and the second one extended from C19′ to C23′. As far as the acyl moiety, the overlapping of a number of methylene signals in the ^{1}H NMR spectrum prevented the delineation of the whole spin sequence; however, key signals relative to protons located at the ends of the alkyl chain clearly indicated its unbranched nature. In particular, a 2H triplet at δ 2.24 (H_2-2), coupled with a methylene quintet at δ 1.53 (H_2-3), was present. This latter signal was in turn coupled with a broad band at δ 1.32 comprising the signals of 11 methylene groups. In the high-field region just one methyl signal was present as a triplet; it resonated at δ 0.89 (3H; H_3-16) and resulted in being coupled with the methylene signal resonating at δ 1.25 (H_2-15); finally, a further correlation between this latter signal and the large signal at δ 1.32 was also observed.

The assembly of the above part structures was made possible through connectivities deduced from the HMBC spectrum around the two unprotonated carbons C-1 (δ 172.8) and C-18′ (δ 93.4). Long-range couplings indicated that the carbonyl group at δ 172.8 was correlated to the methine proton at δ 5.29 (H-

(12) (a) Haines, T. H. *Annu. Rev. Microbiol.* **1973**, *27*, 403. (b) Haines, T. H. In *Lipids and Biomembranes of Eukaryotic Microorganism*; Erwin, J. A., Ed.; Academic Press: New York, 1973; pp 197−232.
(13) Mercer, E. I.; Davies, C. I. *Phytochemistry* **1979**, *18*, 457.
(14) Hansen, J. A. *Physiol. Plant.* **1973**, *29*, 234.
(15) *Gazzetta Ufficiale della Repubblica Italiana*; 1990; No. 211 (Sept 10). *Decreti Ministeriali 1 Agosto*; 1990, Nos. 256 and 257.

Table 1. ^{13}C and ^{1}H NMR Spectroscopic Data of Compounds **1** and **2** (CD_3COCD_3)[a]

compd **1**			compd **2**		
position	δ_H, mult; *J* in Hz	δ_C, mult	position	δ_H, mult; *J* in Hz	δ_C, mult
1	–	174.1	1	–	172.8
2	2.24 m	30.6	2	2.24 t; 7.3	30.6
3	1.53 m; 7.3	25.4	3	1.53 q; 7.3	25.4
4−14	1.32[b]	20.3	4−14	1.32[b]	20.3
15	1.25[b]	20.1	15	1.25[b]	20.1
16	0.89 t; 7.4	14.1	16	0.89 t; 7.4	14.1
1′	5.32 q; 6.5	70.4	1′	5.29 quintet; 6.5	70.5
2′	5.70 dd; 6.3, 15.3	135.1	2′	5.65 dd; 6.5, 15.3	134.3
3′	5.81 dt; 6.6, 15.3	126.8	3′	5.74 dt; 6.6, 6.6, 15.3	127.5
4′	2.83 m	39.0	4′	2.77 m	39.7
5′	4.53[b]	62.4	5′	4.54 m	60.8
6′	4.20 dd; 1.2, 2.8	60.5	6′	4.58 dd; 2.8, 1.2	65.2
7′	4.82[b]	76.3	7′	4.72 ddd; 1.2, 3.3, 9.0	74.3
8′a	2.22 m	38.8	8′a	2.14 m	35.8
8′b	2.53 m		8′b	2.18 m	
9′	4.89[b]	65.7	9′	4.92 ddd; 1.1, 2.0, 9.6	58.6
10′	4.87[b]	58.8	10′	4.61 dd; 2.0, 9.7	66.3
11′	4.41[b]	75.7	11′	5.33 dd; 2.4, 9.7	70.7
12′	4.56[b]	67.6	12′	4.82 dd; 2.4, 8.9	64.7
13′	4.80[b]	65.6	13′	4.42 dd; 1.6, 8.9	62.7
14′	4.38[b]	60.5	14′	5.05 dd; 1.6, 9.5	59.7
15′	4.17 dd; 1.8, 9.5	79.1	15′	5.50 dd; 1.8, 9.5	76.7
16′	5.12 bs	60.9	16′	5.18 br s	57.2
17′	4.22 s	73.8	17′	5.83 s	73.4
18′	–	97.6	18′	–	93.4
19′	2.66 m	39.2	19′	2.55 m	41.1
20′a	2.25 m	38.5	20′a	2.18 m	30.2
20′b	2.54 m		20′b	2.35 m	30.2
21′	4.24[b]	64.6	21′	4.43 ddd; 1.8, 7.5, 1.8	61.2
22′	4.22[b]	69.3	22′	5.36 ddd; 1.8, 4.0, 5.3	72.8
23′a	4.26[b]	63.8	23′a	4.30 m	63.4
23′b	4.01[b]		23′b	4.25 m	
CH_3-1′	1.29[b]	19.8	CH_3-1′	1.27[b]	20.2
			CO-11′	–	171.3
			CO-15′	–	168.3
			CO-17′	–	168.6
			CO-22′	–	170.5
			CO-23′	–	170.3

[a] Assignment based on DEPT, COSY, HMQC, HMBC, and NOE difference experiments. [b] Overlapped with other signals.

Chart 2

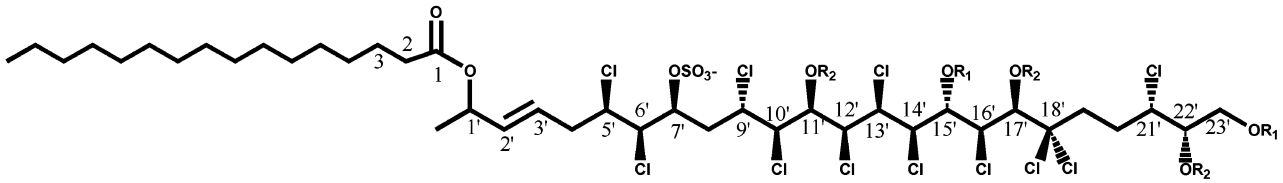

2 $R_1 = R_2 = COCH_3$
3 $R_1 = H$; $R_2 = (S)$-MTPA
4 $R_1 = H$; $R_2 = (R)$-MTPA

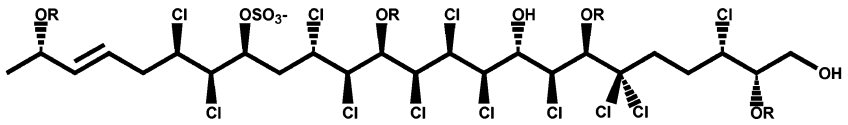

5 R= (*S*)-MTPA

1′), as well as to the first CH_2 of the methylene chain at δ 2.24, thus allowing one to position the ester functionality. The whole of these data, together with the presence of an intense fragment ion at *m*/*z* 255 $[C_{16}H_{31}O_2]^-$ in the mass spectra, indicated a hexadecanoyl moiety attached to carbon 1′. The connection of the remaining two structural units through the carbon atom at δ 93.4 emerged from the long-range $^{1}H-^{13}C$ couplings between this carbon and H-17′ (δ 5.83) and H_2-19′ (δ 2.55), as well as between C-19′ (δ 41.1) and H-17′.

To fully establish the gross structure **2**, it remained to assign the exact location of 17 functional groups (11 chlorines, 5 acetoxyls, and 1 sulfate) on the as many methine groups present in the individuated spin systems. The location of the acetoxy groups at positions 11′, 15′, 17′, 22′, and 23′ was allowed by

inspection of the HMBC spectrum of the acetylated compound, which showed a long-range coupling between the acetyl carbonyl at δ 170.3 with the oxymethylene protons (δ 4.30 and 4.25), while the remaining four acetyl carbonyls at δ 171.3, 170.5, 168.6, 168.3 were long-range coupled with oxymethine protons resonating at δ 5.33, 5.36, 5.83, and 5.50, respectively.

Among the 10 still unassigned sp^3 methine carbons in the ^{13}C NMR spectrum, only one resonates at quite a low field (C-7′, δ 74.3); this pointed to the location of the sulfate group at this position on account of its higher deshielding effect when compared with that of a chlorine atom. Consequently, the eleven chlorines were unequivocally placed: nine on the remaining nine methine groups and two on the only sp^3 unprotonated carbon (C18′; δ 93.4).

Once the planar structure of the peracetyl chlorosulfolipid **2** was secured, the assignment of the ^1H and ^{13}C NMR spectra of the original **1** became a feasible task through a retrospective analysis of the COSY, HOHAHA, ROESY, and HMQC NMR spectra (see Table 1).

Determination of the absolute stereochemistry at the fifteen centers and one stereogenic axis, namely, fifteen chiral carbons and the carbon−carbon double bond, in the chlorosulfolipid **1** appeared particularly challenging. The *E* geometry of the double bond was derived from the large coupling constant (*J* 15.3 Hz) between H-2′ and H-3′. Additional evidence was obtained from the ROESY cross-peaks between H-3′ and H-1′, as well as between H-2′ and H-4′.

As for the chiral carbons, we took advantage of the fact that most of them were adjacent or alternating. So, *J*-based configuration analysis could be successfully applied to our molecule.[16] It is a recently powerful method developed by Murata for the elucidation of relative stereochemistry in acyclic structures using $^3J_{H,H}$ and $^{2,3}J_{C,H}$ values, often in combination with NOE/ROE data. This approach allows the determination of the predominant staggered rotamer(s), with the correct relative configuration, among the six possible staggered conformers of each two-carbon fragment in which a chiral molecule with consecutive or alternating stereogenic centers can be ideally divided.

Using ^1H NMR, HETLOC and PS-HMBC experiments, homonuclear and heteronuclear *J* values of the functionalized portions C5′−C16′ and C21′−C22′ of the molecule were successfully determined (Table 2) and evaluated. It is to be noted that (i) for the stereochemical relationship between the alternating chiral carbon atoms C7′ and C9′, assignment of the diastereotopic methylene C8′ protons were first determined; (ii) for the 1,2-methine systems along C5′−C6′, C6′∠C7′, C9′∠C10′, C11′∠C12′, C13′∠C14′, C15′∠C16′, and C21′∠C22′, as well as the 1,3-methine system along C7′∠C-9′, the coupling constant data were consistent and sufficient to determine their relative configurations; (iii) for the relative stereochemistry of the 1,2-methine systems along C10′∠C11′, C12′∠C13′, and C14′∠C15′ bonds, where a proton−proton anti arrangement is present, $^{2,3}J_{C,H}$ could not be used to distinguish between the two possible rotamers (*threo* or *erythro*). In this case, provided for by Murata method, proximity contacts between protons within a given C_2 fragment are of crucial importance. In fact, for C/C-gauche conformation (*threo* rotamer), the hydrogens linked to the two gauche carbons should come within the range of NOE, while in the case of C/C-anti conformation (*erythro* rotamer), no NOE should be observed between them. In our case, NOE experiments revealed spatial proximity for H-9′ and H-12′ as well as for H-11′ and H-14′, but none for H-13′ and H-16′; in this way we identified the right rotamers along C10′∠C11′ and C12′∠C13′ both as *threo* and along C14′∠C15′ bonds as *erythro*.

In conclusion, the Murata method was successfully applied to all of the C_2 investigated fragments, allowing us to solve the relative configurations of all the stereogenic centers, apart from the C16′∠C17′ bond; so, the configuration of the fragment C5′∠C16′ must be 5′*R*, 6′*R*, 7′*S*, 9′*S*, 10′*R*, 11′*R*, 12′*S*, 13′*S*, 14′*R*, 15′*R*, 16′*S*, or its enantiomer, while the configuration of the fragment C21′∠C22′ must be 21′*S*, 22′*S*′ or its enantiomer.

As far as the assignment of the relative configuration of the segment C16′∠C17′, the observed *J*-values were inconsistent (large ^3J value for C15′∠H17′ and C18′∠H16′ and small ^2J value for C16′∠H17′ and C17′∠H16′). In this regard it has to be underlined that *J*-based configuration analysis is founded on the assumption that 1,2- and 1,3-methine systems take dominant staggered conformation(s). This seems to be quite reasonable for acyclic carbon chains with unbulky substituents, which usually cause no significant deviations from anti or gauche orientation. If this is the case, the homonuclear and heteronuclear couplings are coherent for an unambiguous assignment of the relative configuration. However, when dihedral angles H−H of the dominant rotamers deviate from a staggered conformation by over 10°, $^3J_{H,H}$ becomes an atypical value and unconditional assignment of stereochemistry cannot be achieved, particularly when conformational change is involved. The accurate measurement of $^3J_{H,H}$ (0 Hz) between H-16′ and H-17′, evidenced a dihedral angle consistently deviating from the right one for a staggered conformation. This deviation, which can be attributed to the presence of the bulky $-CCl_2$ group at C-17′, fully accounts for the inconsistency of the observed $^{2,3}J_{C,H}$ data.

To overcome the failed assignment of the C16′∠C17′ relative configuration by Murata method, we take advantage of the presence of an hydroxyl group at C17′; so, we determined the absolute configuration at this position by application of the modified Mosher method suggested by Kakisawa.[17] For this purpose compound **1** was treated with *R*(−) and *S*(+) α-methoxy-α-(trifluoromethyl)phenylacetyl (MTPA) chloride in pyridine solution at room temperature for 2 h to give mixtures of ester derivatives. HPLC purification of the mixture on a silica gel column (1/1 AcOEt/$CHCl_3$ as eluent) allowed us to isolate the three-MTPA ester **3** [from *R*(−)MTPA] and **4** [from *S*(+)-MTPA] (Chart 2), respectively, that were believed to be appropriate for the application of the Mosher method, because of the absence of mutual influence between the three introduced MTPA groups.

In the three-MTPA esters **3** and **4** the Mosher derivatization occurs at three key positions, namely, C11′, C17′, and C22′, so they allowed not only to determine the absolute configuration at C17′ but also to upgrade our knowledge on the two separate fragments C5′∠C16′ and C22′∠C23′ changing their stereochemistries from relative to absolute ones.

^1H NMR resonances of the esters **3** and **4** were assigned by an extensive analysis of 1D and 2D NMR spectra. Significant

(16) (a) Matsumori, N.; Kaneno, D.; Murata, M.; Nakamura, H.; Tachibana, K. *J. Org. Chem.* **1999**, *64*, 866. (b) Murata, M.; Matsuoka, S.; Matsumori, N.; Kaneno, D.; Paul G. K.; Tachibana, K. *J. Am. Chem. Soc.* **1999**, *121*, 870. Wu, M. *J. Am. Chem. Soc.* **2000**, *122*, 12041.

(17) Ohtani, I.; Kusumi, T.; Kashman, Y.; Kakisawa, H. *J. Am. Chem. Soc.* **1991**, *113*, 4092.

Table 2. $^3J_{H,H}$, $^2J_{C,H}$, and $^3J_{C,H}$ of C5′∠C17′ and C21′∠C22′ Portions of Compound **1**

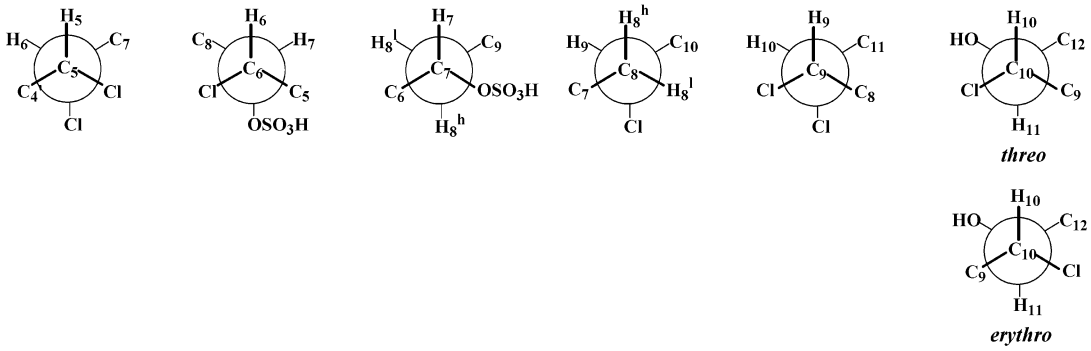

C5-C6 axis	C6-C7 axis	C7-C8 axis	C8-C9 axis	C9-C10 axis	C10-C11 axis
$^3J_{H5\text{-}H6}$ 2.8 Hz (S)	$^3J_{H6\text{-}H7}$ 1.2 Hz (S)	$^3J_{H7\text{-}H8^l}$ 3.3 Hz (S)	$^3J_{H8^h\text{-}H9}$ 1.1 Hz (S)	$^3J_{H9\text{-}H10}$ 2.0Hz (S)	$^3J_{H10\text{-}H11}$ 9.7 Hz (L)
$^3J_{H5\text{-}C7}$ 0 Hz (S)[a]	$^3J_{H6\text{-}C8}$ 1.3 Hz (S)[a]	$^3J_{H7\text{-}H8^h}$ 9.0 Hz (L)	$^3J_{H8^l\text{-}H9}$ 9.6 Hz (L)	$^3J_{H9\text{-}C11}$ 0 Hz (S)[a]	$^3J_{H10\text{-}C12}$ 0 Hz (S)[a]
$^3J_{C4\text{-}H6}$ 0 Hz (S)[a]	$^3J_{C5\text{-}H7}$ 0 Hz (S)[a]	$^3J_{H7\text{-}C9}$ 0 Hz (S)[a]	$^3J_{H8^l\text{-}C10}$ 1.3 Hz (S)[a]	$^3J_{C8\text{-}H10}$ 6.1 Hz(L)[b]	$^3J_{C9\text{-}H11}$ 0 Hz (S)[a]
$^2J_{C5\text{-}H6}$ -1.2 Hz (S)[a]	$^2J_{C6\text{-}H7}$ - 2.2Hz (S)[b]	$^3J_{C6\text{-}H8^h}$ 0 Hz (S)[a]	$^3J_{H8^h\text{-}C10}$ 0 Hz (S)[a]	$^2J_{C9\text{-}H10}$ -5.3 Hz(L)[b]	$^2J_{C10\text{-}H11}$-5.9 Hz (L)[b]
$^2J_{C6\text{-}H5}$ -0.8 Hz (S)[a]	$^2J_{C7\text{-}H6}$ 0 Hz (S)[a]	$^3J_{C6\text{-}H8^l}$ 1.9 Hz (S)[a]	$^3J_{C7\text{-}H9}$ 0 Hz (S)[a]	$^2J_{C10\text{-}H9}$ -1.9 Hz(S)[a]	$^2J_{C11\text{-}H10}$-5.2 Hz (L)[b]
		$^2J_{C7\text{-}H8^l}$ -2.2 Hz (S)[b]	$^2J_{C9\text{-}H8^l}$ -5.0 Hz (L)[b]		
		$^2J_{C7\text{-}H8^h}$ -4.8 Hz(L)[b]	$^2J_{C9\text{-}H8^h}$ -2.3 Hz (S)[b]		

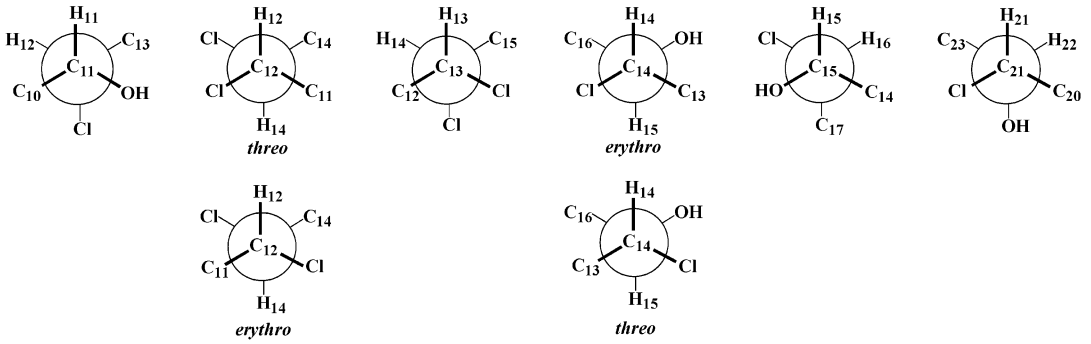

C11-C12 axis	C12-C13 axis	C13-C14 axis	C14-C15 axis	C15-C16 axis	C21-C22 axis
$^3J_{H11\text{-}H12}$ 2.4 Hz (S)	$^3J_{H12\text{-}H13}$ 8.9 Hz (L)	$^3J_{H13\text{-}H14}$ 1.6 Hz (S)	$^3J_{H14\text{-}H15}$ 9.5 Hz (L)	$^3J_{H15\text{-}H16}$ 1.8 Hz (S)	$^3J_{H21\text{-}H22}$ 1.8 Hz (S)
$^3J_{H11\text{-}C13}$ 2.6 Hz (S)[a]	$^3J_{H12\text{-}C14}$ 2.7 Hz (S)[a]	$^3J_{H13\text{-}C15}$ 0 Hz (S)[a]	$^3J_{H14\text{-}C16}$ 2.4 Hz (S)[a]	$^3J_{H15\text{-}C17}$ 7.0 Hz (L)[b]	$^3J_{H21\text{-}C23}$ 0 Hz (S)[a]
$^3J_{C10\text{-}H12}$ 0 Hz (S)[a]	$^3J_{C11\text{-}H13}$ 1.3 Hz (S)[a]	$^3J_{C12\text{-}H14}$ 0 Hz (S)[a]	$^3J_{C13\text{-}H15}$ 2.7 Hz (S)[a]	$^3J_{C14\text{-}H16}$ 3.0 Hz (S)[a]	$^3J_{C20\text{-}H22}$ 1.3 Hz (S)[a]
$^2J_{C11\text{-}H12}$ 0 Hz (S)[a]	$^2J_{C12\text{-}H13}$ -5.7 Hz(L)[b]	$^2J_{C13\text{-}H14}$ -2.2 Hz(S)[a]	$^2J_{C14\text{-}H15}$ -4.6 Hz(L)[b]	$^2J_{C15\text{-}H16}$ -2.1 Hz(S)[a]	$^2J_{C21\text{-}H22}$ 0 Hz (S)[a]
$^2J_{C12\text{-}H11}$ -2.1 Hz(S)[a]	$^2J_{C13\text{-}H12}$ -5.3 Hz(L)[b]	$^2J_{C14\text{-}H13}$ 0 Hz(S)[a]	$^2J_{C15\text{-}H14}$ -5.4 Hz(L)[b]	$^2J_{C16\text{-}H15}$ -4.8 Hz(L)[b]	$^2J_{C22\text{-}H21}$ -2.3 Hz(S)[a]

[a] Coupling constants measured by PS-HMBC. [b] Coupling constants measured by HETLOC.

$\Delta\delta$ values ($\delta_{S-\text{MTPA-ester}}-\delta_{R-\text{MTPA-ester}}$) for the protons near to the derivatized chiral centers C11′, C17′, and C22′ were observed (Figure 1). Inspection of the molecular models of the MTPA esters **3** and **4** indicated that there is no steric hindrance to all the MTPA groups adopting the "ideal conformation" having thrifluoromethyl, ester carbonyl, and carbinol methine proton coplanar. Therefore, the distribution of the $\Delta\delta$ values reported in **1** well reflected the anisotropic effect of the MTPA ester. These results enabled the absolute configurations at C11′, C17′, and C22′ in **1** to be determined as *R, R,* and *S*, respectively.

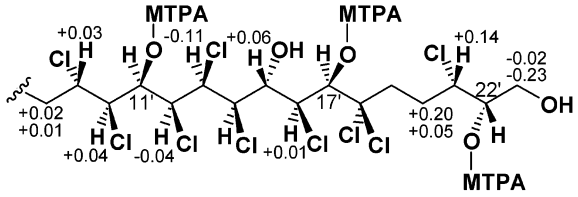

Figure 1. Observed $\Delta\delta$ values ($\delta_S-\delta_R$) in the three-MPTA esters obtained by application of the modified Mosher method for secondary alcohols to compound **1**.

To determine full stereochemistry of **1**, the assignment of the absolute configuration of the isolate asymmetric center at

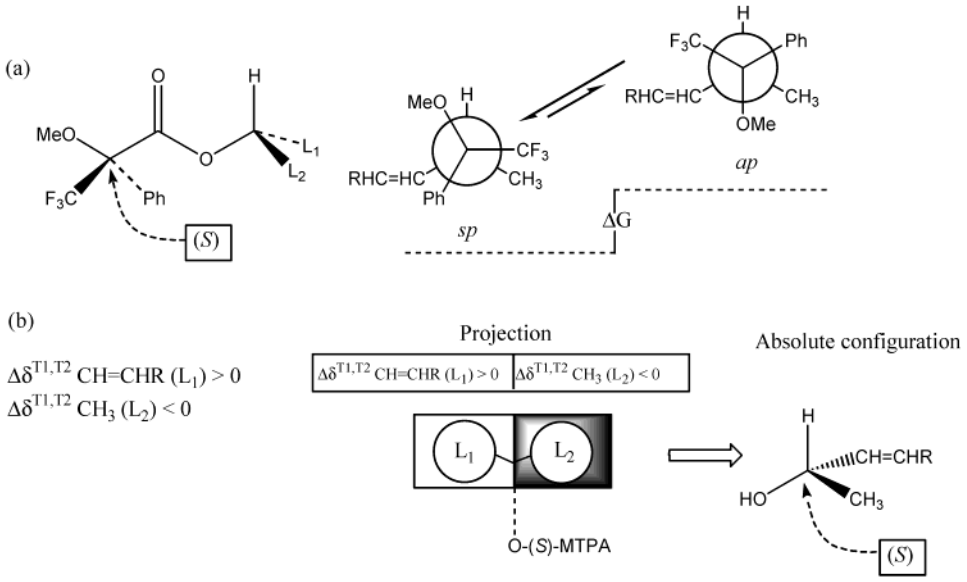

Figure 2. (a) Structure of the sp and ap conformers of the (*S*)-MTPA ester **5**. (b) Scheme to deduce the absolute configuration at C1′ from the experimental $\Delta\delta^{T1,\,T2}$ signs of the (*S*)-MTPA ester **5**.

C1′ was still required. For this purpose we appealed to the Mosher method again. To obtain the required free OH group at C1′, compound **1** was reduced with $LiAlH_4$. The obtained complex mixture, without any further purification, was treated with the Mosher reagent in pyridine solution at room temperature to give a mixture of ester derivatives. Subsequent HPLC purification afforded a very small amount of compound **5** (Chart 2). Due to the low yields of the obtained derivative, as well as of the limited amount of the starting material, we could not repeat the reaction with both enantiomers of the auxiliary reagent. So, we based our analysis on the Reguera's simplified approach of the Mosher method, which requires the use of only one enantiomer [either the (*R*)- or (*S*)-MTPA].[18] The spatial location of substituents around the asymmetric center of the alcohol can be established by comparing the ^{1}H NMR spectra of the ester derivative both at room (T1) and lower (T2) temperatures. At lower temperature, the relative population of the most stable sp conformer is increased and the resonances of the substituents of the alcohol, located under the shielding cone of the phenyl ring, are shifted upfield. At the same time, those protons under the shielding cone in the less populated ap conformer are shifted downfield (see Figure 2).

Two groups of signals were individuated in the ^{1}H NMR spectrum of the (*S*)-MTPA ester **5**, the first formed by the methyl signal that moved downfield in the low-temperature spectrum [negative $\Delta\delta^{T1,T2}$: L_2]; the second group formed by signals that shift upfield in the spectrum recorded at low temperature [positive $\Delta\delta^{T1,T2}$: L_1] (Figure 2). The obtained results suggested the *S* configuration at C1′.

Bearing in mind the relative stereochemistries established by *J*−based configuration analysis and the absolute configurations at C11′, C17′, C22′, and C1′, established by the Mosher method, the whole absolute configuration of the molecule was consequently assigned as 1′*S*, 5′*R*, 6′*R*, 7′*S*, 9′*S*, 10′*R*, 11′*R*, 12′*S*, 13′*S*, 14′*R*, 15′*R*, 16′*S*, 17′*R*, 21′*S*, 22′*S*.

Compound **1** was tested for its antiproliferative activity on WEHI 164 (murine fibrosarcoma) and RAW 274.7 (murine monocyte/macrophage) cell lines, and it was found to inhibit the growth of both cell lines evaluated at 72 h with an IC_{50} of 13.5 and 20 μg/mL, respectively.

Chlorosulfolipid **1** is unique among natural products as it possesses a dense functionalization of the alkenyl chain with eleven secondary chlorines, five hydroxyl groups, and one sulfate group. As a class, chlorosulfolipids have been found to be responsible for the antibiotic activity associated with the extracts of several Chrysophyte species.[14] This may be relevant to the ecological role of these amphipatic lipids. Moreover, the recurring finding of polychlorinated sulfolipids in Adriatic mussels represents a further alarm for shellfish consumers. Of course, it remains to be identified the sources of this group of compounds and, chiefly, to be clarified their toxicological effects.

Experimental Section

General Methods. ^{1}H (500 MHz) and ^{13}C NMR (125 MHz) spectra were measured on a Bruker AMX-500 spectrometer; chemical shifts are referenced to the residual solvent signals (CD_3COCD_3, $\delta_H = 2.05$ and $\delta_C = 205.7$ and 29.8; CD_3OD, $\delta_H = 3.34$). Methyl, methylene, and methine carbons were distinguished by a DEPT experiment. Homonuclear ^{1}H connectivities were determined by using COSY experiment. One bond heteronuclear ^{1}H−^{13}C connectivities were determined with the Bax and Subramanian HMQC pulse sequence.[19] Two and three bond ^{1}H−^{13}C connectivities were determined by HMBC experiments optimized for $^{2,3}J = 10$ Hz. The 2D hetero half-filtered TOCSY (HETLOC) experiment[20] was determined on a Bruker DRX-600 spectrometer. Low- and high-resolution ESIMS (negative ion mode) were performed by M-Scan S. A. (12, chemin des Aulx, 1228 Plan-les-Ouates, Switzerland) on a VG Analytical ZAB 2SE high-field mass spectrometer. Negative ESI MSMS was carried out with a Thermofinnigan LCQ MAT (ion trap) mass spectrometer. Medium-pressure liquid chromatographies (MPLC) were performed on a Büchi 861 apparatus using RP-18 (40−63 μm) stationary phase.

Isolation of 1. Chlorosulfolipid **1** was isolated from acetone extracts of contaminated shellfish (*Mytilus galloprovincialis*) digestive glands (total 1.2 kg dry weight) collected in October 1999 from one sampling

(18) Latypov, S. K.; Seco, J. M.; Quinoà, E.; Riguera, R. *J. Am. Chem. Soc.* **1998**, *120*, 877.

(19) Bax, A.; Subramanian, S. *J. Magn. Reson.* **1986**, *67*, 565.

(20) Kurz, M.; Schmieder, P.; Kessler, H. *Angew. Chem., Int. Ed. Engl.* **1991**, *30*, 1329.

site located along the Emilia Romagna coasts of Italy, following procedures closely parallel to those described previously.[10] The digestive glands were found toxic by the mouse bioassay method for DSP.[11] The digestive glands were extracted two times with acetone, and after evaporation the residue was extracted thrice with EtOAc. The extracts obtained after removal of the solvent were dissolved in 80% MeOH and partitioned against *n*-hexane. Subsequently, the MeOH layer was diluted to 40% MeOH and further partitioned against CH_2Cl_2. The dichloromethane toxic residue was fractionated by repeated bioassay-guided column chromatography on ODS (aqueous MeOH) and successively on TOYOPEARL (MeOH). The final HPLC purification was carried out on a RP 18 column with 7/3 CH_3OH/H_2O as eluent, thus obtaining 6.2 mg of pure compound **1**: $[\alpha]^{25}_D$ +120.2 (c = 0.0048, MeOH); ^{1}H and ^{13}C NMR (CD_3COCD_3) data are reported in Table 1; IR (KBr) ν_{max} 1240, 1220, and 820 cm^{-1}; ESIMS (negative ion mode) m/z 1139, 1141, 1143, 1145, 1147, 1149, 1151; HRESIMS m/z 1141.0936 ($C_{40}H_{66}O_{11}S\ ^{35}Cl_{10}{}^{37}Cl$ requires 1141.0870).

Acetylation of 1. A 3 mg amount of **1** was treated with Ac_2O in anhydrous pyridine for 12 h, thus obtaining 3.2 mg of peracetylated **2**. ^{1}H and ^{13}C NMR (CD_3COCD_3) data are reported in Table 1; IR (KBr) ν_{max} 1240, 1220, and 820 cm^{-1}; ESIMS (negative ion mode) m/z 1349, 1351, 1353, 1355, 1357, 1359, 1361.

Preparation of the (*R*)- and (*S*)-MTPA Esters of 1. Compound **1** (0.8 mg) was dissolved in anhydrous pyridine (200 μL), treated with 5 μL of (*R*)-MTPA chloride [MTPA = α-methoxy-α-(trifluoromethyl)-phenylacetyl], and 4-(dimethylamino)pyridine (DMAP, a spatula tip), and then maintained at room temperature for 2 h, while stirring. H_2O (5 mL) and solid K_2CO_3 were then added, and the solution was extracted with $CHCl_3$ (5 mL). The organic phase, after evaporation of the solvent, yielded a mixture of ester derivatives. HPLC purification of the mixture on a silica gel column (1/1 AcOEt/$CHCl_3$ as eluent) allowed us to isolate the (*S*)-MTPA triester **3**. The use of (*S*)-MTPA chloride in the same procedure led to the (*R*)-MTPA triester **4**.

Compound 3. Selected ^{1}H NMR chemical shifts (CD_3OD): H_2-8′ δ 2.74, 2.37; H-9′ δ 4.24; H-10′ δ 4.44; H-11′ δ 5.83; H-12′ δ 4.59; H-13′ δ 4.84; H-15′ δ 4.63; H-16′ δ 4.94; H-17′ δ 6.37; H_2-20′ δ 2.58, 2.77; H-21′ δ 4.24; H-22′ δ 5.78; H_2-23′ δ 4.39, 3.96.

Compound 4. Selected ^{1}H NMR chemical shifts (CD_3OD): H_2-8′ δ 2.72, 2.33; H-9′ δ 4.21; H-10′ δ 4.40; H-11′ δ 5.78; H-12′ δ 4.63; H-13′ δ 4.95; H-15′ δ 4.57; H-16′ δ 4.93; H-17′ δ 6.38; H_2-20′ δ 2.38, 2.72; H-21′ δ 4.10; H-22′ δ 5.84; H_2-23′ δ 4.41, 4.19.

Reduction of 1. Chlorosulfolipid **1** (1.0 mg, 7.02 × 10^{-4} mmol) was dissolved in dry diethyl ether (5 mL), and $LiAlH_4$ ether solution (3.5 × 10^{-3} mmol) was added to the solution. The reaction mixture was kept at 50 °C for 2.5 h while stirring. After adding EtOAc (3 mL), the solution was initially concentrated in vacuo, then solved in water, and finally partitioned with $CHCl_3$. The organic phase was concentrated and afforded 0.8 mg of a complex mixture**.**

Preparation of the (*S*)-MTPA Ester 5. The mixture (0.8 mg) obtained after reduction of **1** was dissolved in anhydrous pyridine (200 μL), treated with 5 μL of (*R*)-MTPA chloride, and then allowed to react at room temperature for 2 h, while stirring. H_2O (5 mL) and solid K_2CO_3 were then added, and the solution was extracted with $CHCl_3$ (5 mL). The organic phase, after evaporation of the solvent, yielded a mixture of (*S*)-MTPA esters. HPLC purification of the mixture on a silica gel column (1/1 AcOEt/$CHCl_3$ as eluent) led to the isolation of the (*S*)-MTPA ester **5**.

Compound 5. Selected ^{1}H NMR chemical shifts (CD_3OD; room temperature): CH_3-1′ δ 1.46; H-1′ δ 5.13; H-2′ δ 6.07; H-3′ δ 6.12. Selected ^{1}H NMR chemical shifts (CD_3OD; low temperature, 243 K): CH_3-1′ δ 1.49; H-1′ δ 5.15; H-2′ δ 5.98; H-3′ δ 6.09.

Cytotoxicity Assay. WEHI 164 cells (murine fibrosarcoma cell line) were maintained in adhesion with Dulbecco's Modified Eagle's Medium (DMEM) supplemented with 10% heat-inactivated fetal bovine serum (FBS), 25 mM HEPES, penicillin (100 U/mL), streptomycin (100 μg/mL), and 2 mM L-glutamine. RAW 264.7 cells (murine monocyte/macrophage cell line) were grown in adhesion on Petri dishes with DMEM medium supplemented with 10% FBS, 25 mM Hepes, penicillin (100 U/mL), streptomycin (100 μg/mL), and 2 mM L-glutamine. All reagents for cell culture were from Biowhittaker. MTT [3-(4,5-dimethylthiazol-2-yl)-2,5-phenyl-2*H*-tetrazolium bromide] was from Sigma.

WEHI 164, J774, and P388 (1 × 10^4 cells) were plated on 96-well plates in 50 μL and allowed to adhere at 37 °C in 5/95 CO_2/ air for 2 h. Thereafter the medium was replaced with 50 μL of fresh medium and 50 μL of 1/4 v/v serial dilution of the test compound **1** was added and then the cells were incubated for 72 h. The cells viability was assessed through an MTT conversion assay.[21] Briefly, after 72 h of incubation, 25 μL of MTT (5 mg/mL) were added to each well and the cells were incubated for additional 3 h. Following this time the cells were lysed and the dark blue crystal solubilized with 100 μL of a solution containing 50% (v/v) *N*,*N*-dimethylformamide and 20% (v/v) SDS with an adjusted pH of 4.5.[22] The optical density (OD) of each well was measured with a microplate spectrophotometer equipped with a 620 nm filter. The viability of each cell line in response to treatment with compound **1** was calculated as follows: % dead cells = 100 − (OD treated/OD control) × 100. The results are expressed as IC_{50} (the concentration that inhibited the cell growth by 50%).

Acknowledgment. This work is dedicated to the memory of Prof. Guido Sodano. It is a result of a research supported by MURST PRIN "Chimica dei Composti Organici di Interesse Biologico", Rome, Italy. NMR and FABMS spectra were performed at "Centro di Ricerca Interdipartimentale di Analisi strumentale", Università degli studi di Napoli "Federico II".

Supporting Information Available: compound **1** spectra (^{1}H NMR, ^{1}H-^{1}H COSY, ^{1}H-^{13}C HMQC, HRESIMS) and compound **2** spectra (^{1}H NMR,^{13}C NMR, DEPT, ^{1}H-^{1}H COSY, HOHAHA, ^{1}H-^{1}H ROESY,^{1}H-^{13}C HMQC, ^{1}H-^{13}C HMBC, ^{1}H-^{13}C PSH-MBC, HETLOC) (all the spectra were recorded in CD_3COCD_3) (PDF). This material is available free of charge via the Internet at http://pubs.acs.org.

JA0207347

(21) Mosmann, T. *J. Immunol. Methods* **1983**, *65*, 55.
(22) Opipari, A. W., Jr.; Hu, H. M.; Yabkowitz, R.; Dixit, V. M. *J. Biol. Chem.* **1992**, *267*, 12424.